

Synthesis, characterization and magnetic investigation of $(\text{NH}_4)_{0.5}\text{Mn}_{1.25}(\text{H}_2\text{O})_2[\text{BP}_2\text{O}_8]\cdot 0.5\text{H}_2\text{O}$

B. Birsöz¹, A. Baykal^{1*}, M. Toprak², Y. Köseoglu³

¹ Department of Chemistry,
Fatih University,
B.Çekmece, 34500 Istanbul, Turkey

² Department of Chemistry and Biochemistry,
University of California,
Santa Barbara, CA 93106, USA

³ Department of Physics,
Fatih University,
B.Çekmece, 34500 Istanbul, Turkey

Received 19 October 2006; accepted 13 December 2006

Abstract: A new borophosphate compound with the composition $(\text{NH}_4)_x\text{Mn}_{(3-x)/2}(\text{H}_2\text{O})_2[\text{BP}_2\text{O}_8]\cdot(1-x)\text{H}_2\text{O}$ was prepared under mild hydrothermal conditions and characterized by X-ray powder diffraction (XRD) and Fourier Transform Infrared Spectroscopy (FTIR) methods. The title compound was synthesized from $\text{MnCl}_2\cdot 2\text{H}_2\text{O}$, H_3BO_3 , and $(\text{NH}_4)_2\text{HPO}_4$ with variable molar ratios by heating at 180 °C for 7 days in an autoclave. The X-ray diffraction data of the water insoluble polycrystalline powder was indexed using the TREOR program in hexagonal system with the unit cell parameters of $a = 9.5104$, $c = 15.7108$ Å, $Z = 6$ and the space group P6_5 (No.176). $(\text{NH}_4)_x\text{Mn}_{(3-x)/2}(\text{H}_2\text{O})_2[\text{BP}_2\text{O}_8]\cdot(1-x)\text{H}_2\text{O}$ is isostructural with $(\text{NH}_4)_x\text{M}_{(3-x)/2}^{II}(\text{H}_2\text{O})_2[\text{BP}_2\text{O}_8]\cdot(1-x)\text{H}_2\text{O}$ ($\text{M}^{II} = \text{Co}, \text{Cd}, \text{Mg}; x = 0.5-1$). Its unit cell parameters and hkl values were in good agreement with the other isostructural compounds. This is the first report presenting both the synthetic details and the indexed X-ray powder diffraction pattern of this compound along with the characterization by FTIR, thermal gravimetric analysis, scanning electron microscopy and EPR.

© Versita Warsaw and Springer-Verlag Berlin Heidelberg. All rights reserved.

Keywords: Borophosphate, molecular sieve, microporous, hydrothermal synthesis, EPR

* E-mail: hbaykal@fatih.edu.tr

1 Introduction

Alkaline earth, rare earth and transition metal borophosphate compounds have been studied and investigated in detail in recent years [1–4]. Compounds with open-framework structures are of great interest in material science, as well as in chemistry, due to their applications as catalysts, ion-exchangers, or molecular sieves [5–7]. Open-framework borophosphates are potential materials for heterogeneous catalysis, as well established for BPO_4 [8, 9]. Although systematic investigations on borophosphates began only a few years ago, a broad spectrum of compounds has already been characterized with various anionic partial structures such as oligomeric units, chains, ribbons, layers, and three-dimensional frameworks [10–13]. The possibility of creating more open structures by using organic templates was also demonstrated [14–16].

Molecular sieve compounds are a class of crystalline solids which, because of their porous nature, have a wide variety of uses for both catalytic and adsorption purposes [17]. Since BPO_4 itself is an effective catalyst in a variety of dehydration, hydration, alkylation, oligomerization and rearrangement reactions, incorporation of borophosphate groups into microporous metal-borophosphates offers the potential for enhanced catalytic efficiency, as well as hydrolytic stability and the additional catalytic activity of the metal centers of the framework [18, 19]. A first approach to an isostructural chemistry of borophosphates was proposed by Kniep et al. [10] in which the crystal structure of borophosphates are first divided into anhydrous and hydrated phases. According to this classification, hydrated borophosphates with a molar ratio of B:P=1 and B:P<1 are exclusively built of borate and phosphate tetrahedra and do not contain boron in a trigonal planar coordination.

Many compounds in the series of borophosphates with formula $\text{M}_x^I\text{M}_y^{II}(\text{H}_2\text{O})_2[\text{BP}_2\text{O}_8] \cdot z\text{H}_2\text{O}$ ($\text{M}^I = \text{Li}^+, \text{Na}^+, \text{K}^+, \text{Rb}^+, \text{Cs}^+$; $\text{M}^{II} = \text{Mg}^{2+}, \text{Mn}^{2+}, \text{Fe}^{2+}, \text{Co}^{2+}, \text{Ni}^{2+}, \text{Cu}^{2+}, \text{Zn}^{2+}$; $x = 0.35-1$, $y = 1-1.3$, $z = 0.2-1$) have been reported [20]. However, there only a few of these compounds contain NH_4^+ ion, namely $(\text{NH}_4)_{0.4}\text{Fe}_{0.55}^I\text{Fe}_{0.5}^{II}(\text{H}_2\text{O})_2[\text{BP}_2\text{O}_8] \cdot 0.6\text{H}_2\text{O}$ [21], $(\text{NH}_4)_x\text{Co}_{(3-x)/2}(\text{H}_2\text{O})_2[\text{BP}_2\text{O}_8] \cdot (1-x)\text{H}_2\text{O}$ ($x \approx 0.5$) [22], $\text{NH}_4\text{Cd}(\text{H}_2\text{O})_2[\text{BP}_2\text{O}_8] \cdot 0.72\text{H}_2\text{O}$ [7], and $\text{NH}_4\text{Mg}(\text{H}_2\text{O})_2[\text{BP}_2\text{O}_8] \cdot \text{H}_2\text{O}$ [23]. Furthermore, $\text{NH}_4\text{Mn}(\text{H}_2\text{O})_2[\text{BP}_2\text{O}_8] \cdot \text{H}_2\text{O}$ is the first example of a borophosphate containing both Mn and NH_4^+ . Here, we report the synthesis and characterization of the new borophosphate $(\text{NH}_4)_{0.5}\text{Mn}_{1.25}(\text{H}_2\text{O})_2[\text{BP}_2\text{O}_8] \cdot 0.5\text{H}_2\text{O}$ in the $\text{M}_x^I\text{M}_y^{II}(\text{H}_2\text{O})_2[\text{BP}_2\text{O}_8] \cdot z\text{H}_2\text{O}$ family [7].

2 Experimental

All reagents were obtained from Merck/Sigma-Aldrich and were used as received. The title compound was synthesized under mild hydrothermal conditions starting with the precursor mixture as follows: 4.876 g $\text{MnCl}_2 \cdot 2\text{H}_2\text{O}$, 0.744 g H_3BO_3 , 2.384 g $(\text{NH}_4)_2\text{HPO}_4$ and 15 mL HCl were mixed in 15 g of distilled water and treated under stirring until components dissolved completely. The clear solutions were heated without boiling to reduce the volume to about 12 mL then transferred to teflon autoclaves (degree of filling was 65%) and heated at 180 °C for 7 days. The single phase, pale pink, high yield

products were filtered off in a vacuum, washed with distilled water and dried at 65 °C. This experiment was repeated two times to check the reproducibility of the product under the same conditions.

2.1 Instrumentation

Inductively coupled plasma (ICP) atomic emission spectroscopy was used for the elemental analysis of the prepared sample using Perkin Elmer Optima 4300 DV type ICP instrument and the nitrogen content was analyzed with a carrier gas hot reaction method (LECO, CHNS-932).

X-ray powder diffraction analysis, XRD, was used to characterize the crystalline products with a Huber JSO-DEBYEFLEX 1001 diffractometer using a Cu K α source.

For FTIR measurements, a Mattson satellite FTIR spectrophotometer was used in the region 400–4000 cm $^{-1}$. Spectra of solid samples were obtained from KBr pellets, KBr/sample ratio = 100 mg/3 mg.

Thermal gravimetric analysis (TGA) was used to assess the thermal decomposition behavior of the sample using a NETZCH STA 409 system.

Scanning electron microscopy (SEM) analysis was performed, in order to investigate the microstructure and morphology of the sample, using an FEI XL40 Sirion FEG Digital Scanning Microscope. Samples were coated with gold at 10 mA for 2 min prior to SEM analysis.

A conventional X-band ($f \approx 9.5$ GHz) Bruker EMX model EPR spectrometer employing an AC magnetic field (100 kHz) modulation technique with a cylindrical TE $_{011}$ cavity was used to record the first derivative absorption signal. The powder sample was placed into a quartz sample holder tube and inserted into the cavity. EPR spectra were obtained by sweeping the magnetic field from 0 to 16 kOe. The magnetic field was calibrated using an α , α -diphenyl- β -picryl hydrazyl (DPPH) sample ($g = 2.0036$). The field derivative of microwave power absorption, dP/dH , was registered as a function of DC magnetic field H . To obtain the intensity of microwave power absorption, P , digital integration of the EPR curves was performed by using Bruker WinEPR software.

3 Results and discussion

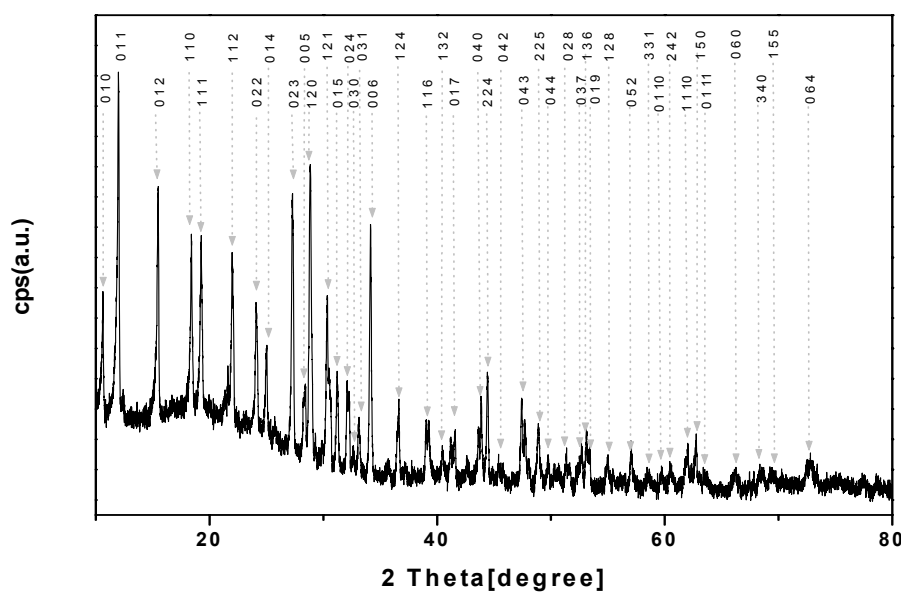
The elemental analysis results of the sample are listed in Table 1 and composition calculations based on these values confirm the title compound with $x = 0.5$, $(\text{NH}_4)_x\text{Mn}_{(3-x)/2}(\text{H}_2\text{O})_2[\text{BP}_2\text{O}_8] \cdot (1-x)\text{H}_2\text{O}$. The results are listed in Table 1 and composition calculations based on these values confirm the composition of the title compound with $x = 0.5$, $(\text{NH}_4)_{0.5}\text{Mn}_{1.25}(\text{H}_2\text{O})_2[\text{BP}_2\text{O}_8] \cdot 0.5\text{H}_2\text{O}$.

The obtained product in the powder form was analyzed by XRD to reveal its crystalline content and crystal structure. The XRD pattern, given in Fig. 1, was indexed using the TREOR program yielding a hexagonal system with the unit cell parameters of $a = 9.5104$, $c = 15.7108$ Å, $Z = 6$ and the space group P6 $_5$ (No.176). According to the

Table 1 Elemental Analysis Results of $(\text{NH}_4)_x\text{Mn}_{((3-x)/2)}(\text{H}_2\text{O})_2[\text{BP}_2\text{O}_8] \cdot (1-x)\text{H}_2\text{O}$ ($x = 0.5$).

	Manganese %	Boron %	Nitrogen %	Phosphorous %
Theoretical	21.2	3.4	2.2	19.1
Experimental	20.9	3.5	1.9	20.1

crystal model done by Kniep et al. [17], the condensation of PO_4 and BO_4 tetrahedra through common vertices leads to tetrahedral ribbons $^{1/\alpha}[\text{BP}_2\text{O}_8]^{3-}$, which are arranged around 6_1 screw axes to form helices. The spiral ribbons are built from four rings of tetrahedra in which the BO_4 and PO_4 groups alternate. Each BO_4 tetrahedron also belongs to the adjacent four-ring tetrahedra along the ribbon, in such a way that all vertices of the BO_4 groups participate in bridging functions with PO_4 tetrahedra as shown in Kniep et al. [22, 23].

**Fig. 1** X-ray powder diffraction pattern of $(\text{NH}_4)_{0.5}\text{Mn}_{1.25}(\text{H}_2\text{O})_2[\text{BP}_2\text{O}_8] \cdot 0.5\text{H}_2\text{O}$ washed with hot H_2O .

Infrared analysis of the product, presented in Fig. 2, showed two bands at 3354 cm^{-1} and 3558 cm^{-1} that can be assigned to water molecules occupying different positions in the structure. The band at 3558 cm^{-1} is due to hydrogen bonding between the hydrated molecules and the other at 3354 cm^{-1} shows the bond between anion and coordinated water. The absence of a band for P-O-P (at around 740 cm^{-1}) is in agreement with the postulate by Kniep et. al. [10] that P-O-P linkages in borophosphate compounds will be absent. The stretching modes of a free PO_4^{3-} anion with T_d symmetry has four internal modes of vibrations [24–27], $\nu_3(\text{PO}_4) = 1107, 1024\text{ cm}^{-1}$, $\nu_1(\text{PO}_4) = 954$, $\nu_4(\text{PO}_4) = 576$, and $\nu_2 = 482\text{ cm}^{-1}$ that are also observed in the IR spectra of the product. The

presence of peaks in the FTIR spectra of the product between $850\text{--}1200\text{ cm}^{-1}$ proves B-O stretching of BO_4 units [8]. FTIR spectra of the product confirms the presence of O-H and N-H vibrations by the following absorption bands with assignments: O-H stretching 3482 cm^{-1} , $\nu_3(\text{N-H})$ (3267 cm^{-1}), O-H deformation (1643 cm^{-1}), and ν_4 (N-H) (1448 cm^{-1}). These assignments verify the presence of NH_4^+ ions which are necessary for the charge balance together with the manganese present in mixed states, as already suggested by the product color alone.

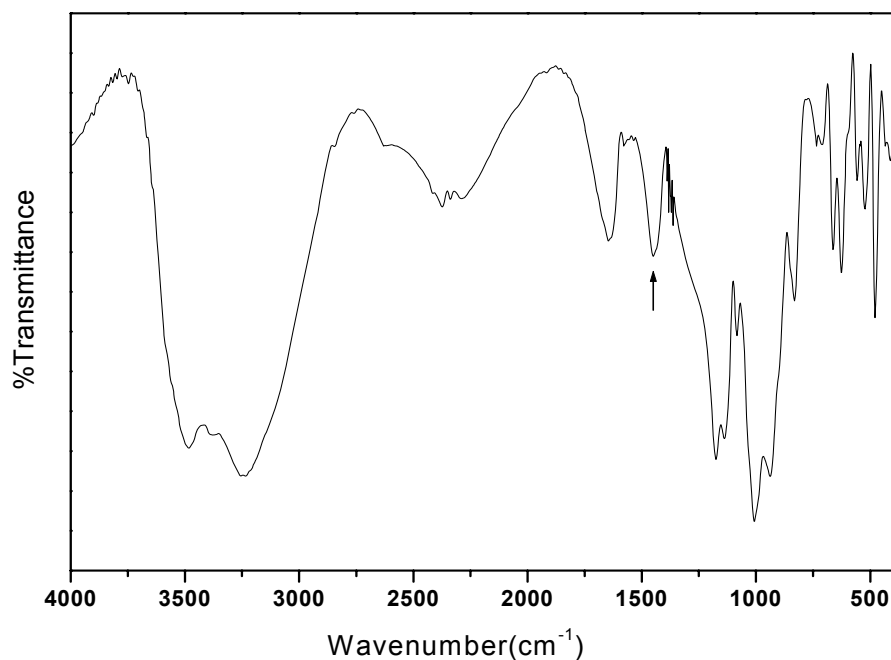


Fig. 2 FTIR spectra of $(\text{NH}_4)_{0.5}\text{Mn}_{1.25}(\text{H}_2\text{O})_2[\text{BP}_2\text{O}_8]\cdot 0.5\text{H}_2\text{O}$. The position of the ν_4 N-H deformation vibration is marked with arrow.

The thermal stabilities of compounds were analyzed by TGA as shown in Fig. 3. Thermal dehydrations of the compound takes place in several steps. In the first step evaporation of adsorbed water is observed around $100\text{ }^\circ\text{C}$. Around $270\text{ }^\circ\text{C}$ crystalline water and 1 mol water coordinated to metal center were released, thereafter the last mole of water in the coordination was lost at $360\text{ }^\circ\text{C}$. The final loss around $560\text{ }^\circ\text{C}$ is assigned to the decomposition of ammonia in the structure.

The morphology and microstructure of the product were investigated by SEM. Typical micrographs are presented in Fig. 4. There are highly faceted crystals in the form of elongated hexagonal bipyramids, Fig. 4(a). These crystals have lengths in the range $2\text{--}5\text{ }\mu\text{m}$ and widths in the range $1\text{--}2.5\text{ }\mu\text{m}$. Overall, the micrographs show the same polygonal crystal form with different sizes, mostly as intergrown twins. In some parts spherical particles in the range $100\text{--}150\text{ nm}$ were observed that were beginning to sinter and probably fuse to already existing crystals, Fig. 4(b). Since the growth takes place via the formation of these polygonal crystals it is hard to estimate a grain size for this system.

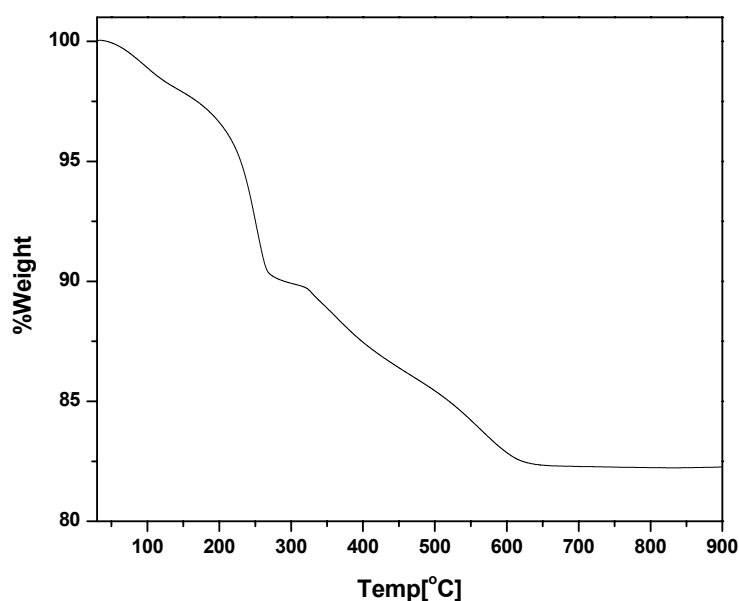


Fig. 3 TGA analysis showing the thermal behavior of $(\text{NH}_4)_{0.5}\text{Mn}_{1.25}(\text{H}_2\text{O})_2[\text{BP}_2\text{O}_8]\cdot 0.5\text{H}_2\text{O}$.

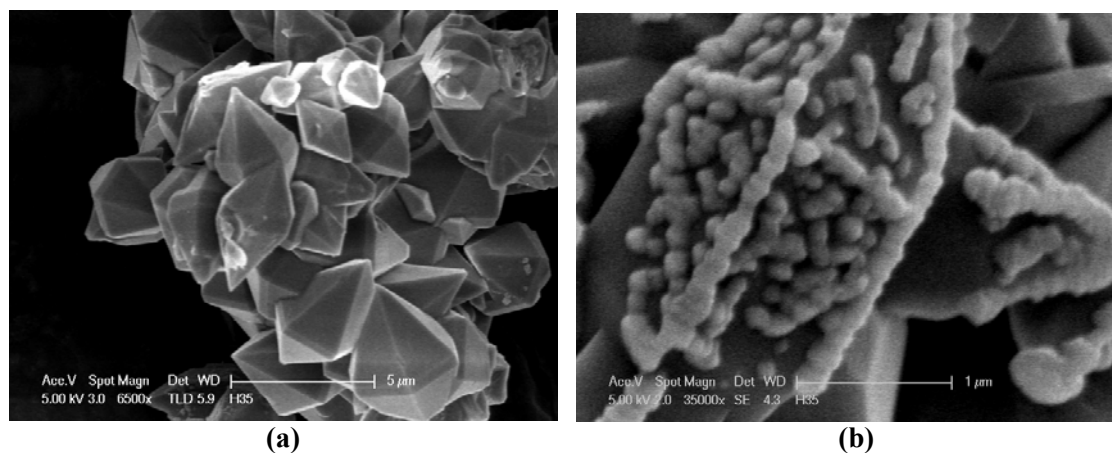


Fig. 4 Typical SEM micrographs of the pale pink coloured phase $(\text{NH}_4)_{0.5}\text{Mn}_{1.25}(\text{H}_2\text{O})_2[\text{BP}_2\text{O}_8]\cdot 0.5\text{H}_2\text{O}$ showing (a) elongated hexagonal bipyramidal crystals, and (b) spherical nanoparticles.

EPR is able to detect paramagnetically isolated species and gives information about the coordination of isolated sites, therefore it can be used to detect Mn^{2+} and Mn^{4+} , whereas Mn^{3+} is usually not detected due to complete splitting of energy levels (no ground-state degeneracy) [28, 29]. Normally, it is expected that any electron paramagnetic (EPR) spectrum, coming from the transitions between the electronic magnetic states ($|M_s\rangle \rightarrow |M_s-1\rangle$), to split into 6 hyperfine components separated about 90–110 G from each other. If the intrinsic line width is larger than this splitting, then the six components overlap producing a broader (at least 500–600 G) single line. Fig. 5 shows the

EPR spectrum of the product that has been measured by varying external magnetic field. A strong and broad microwave resonance absorption signal is observed which reveals the collective behavior of magnetic spins without hyperfine splittings (with approximately isotropic Lande factor $g = 2.040$; which is close to the g -value of the free electron of 2.0023, and peak-to-peak line width = 515 G) at X-band at room temperature. The measured spectrum corresponds to a typical signal of Mn^{2+} as a g value of about 2 is commonly expected for S state ions like Mn^{2+} ($S=5/2$) [30].

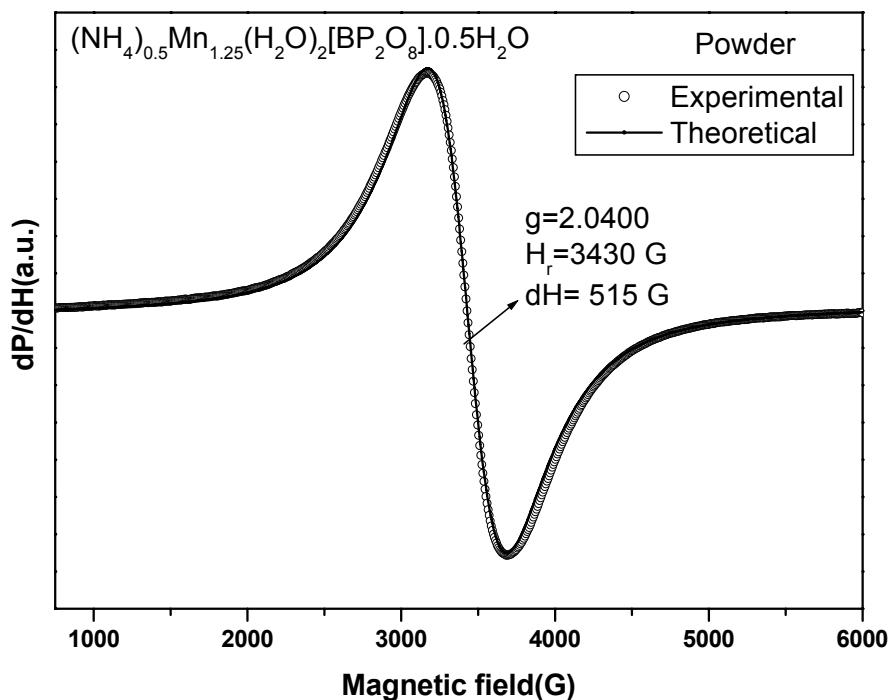


Fig. 5 X-band EPR spectra and its theoretical simulation by using Win-EPR program.

4 Conclusion

In this study, a novel borophosphate compound with the formula $(\text{NH}_4)_x\text{Mn}_{(3-x)/2}(\text{H}_2\text{O})_2[\text{BP}_2\text{O}_8] \cdot (1-x)\text{H}_2\text{O}$ was synthesized by a mild hydrothermal route. Its X-ray powder data and indexing as well as IR analysis confirmed its composition and structure. SEM analysis of the water insoluble product revealed the formation of crystals in the form of elongated hexagonal bipyramids. EPR measurements, showed a strong and broad microwave resonance absorption signal at room temperature indicating the collective behavior of magnetic spins without hyperfine splittings at X-band revealing the presence of Mn^{2+} . This material is the first example of a borophosphate containing both Mn^{2+} and NH_4^+ . This class of borophosphate may find applications as catalysts, ion-exchangers, or molecular sieves due to its open-framework structure.

Acknowledgment

This work was supported by the Project No. P50020402 by Fatih University. Dr. M. Toprak acknowledges the fellowship from Knut och Alice Wallenbergs Foundation (No:UAW2004.0224). The authors would like to thank Prof. Bekir Aktaş (from Gebze High Institute of Technology) for EPR measurements.

References

- [1] A. Baykal: *in PhD Thesis*, Middle East Technical University, Ankara/TURKEY, 1999.
- [2] G. Gözel, A. Baykal, M. Kızılyallı and R. Kniep: “Solid-State Synthesis, X-ray Powder Investigation and IR Study of α -Mg₃[BPO₇]”, *J. Eur. Ceram. Soc.*, Vol. 18, (1998), pp. 2241–2246.
- [3] A. Baykal, G. Gözel, M. Kızılyallı, M. Toprak and R. Kniep: “X-ray Powder Diffraction and IR Study of CaBPO₅”, *Turk. J. Chem.*, Vol. 24, (2000), pp. 381–388.
- [4] A. Baykal, M. Kızılyallı, G. Gözel and R. Kniep: “Synthesis of Strontium Borophosphate, SrBPO₅ by Solid state and Hydrothermal Methods and Characterization”, *Cryst. Res. Technol.*, Vol. 35, (2000), pp. 247–254.
- [5] A.K. Cheetham, G. Ferey and T. Loiseau: “Open-Framework Inorganic Materials”, *Angew. Chem.*, Vol. 38, (1999), pp. 3268–3292.
- [6] A. Yilmaz, L. Tatar Yıldırım, X. Bu, M. Kızılyallı and G.D. Stucky: “New Zeotype Borophosphates with Chiral Tetrahedral Topology: (H)_{0.5}M_{1.25}(H₂O)_{1.5}[BP₂O₈]·H₂O (M= Co(II) and Mn(II))”, *Cryst. Res. Technol.*, Vol. 40(6), (2005), pp. 579–585.
- [7] M. Ge, W. Liu, H. Chen, M. Li, X. Yang and J. Zhao: “NH₄Cd(H₂O)₂(BP₂O₈)·0.72H₂O: a New Borophosphate with Abnormal Structure Changes Caused by Hydrogen Interactions”, *Z. Anorg. Allg. Chem.*, Vol. 631, (2005), pp. 1213–1217.
- [8] G.J. Hutchings, I.D. Hudson and D.G. Timms: “Reactivation of Boron Phosphate Catalysts for the Synthesis of Isoprene from 2-Methylbutanal Dehydration”, *J. Chem. Soc., Chem. Comm.*, Vol. 23, (1994), pp. 2717–2718.
- [9] A. Baykal, M. Kızılyallı, M. Toprak and R. Kniep: “Hydrothermal and Microwave Synthesis of BPO₄”, *Turk. J. Chem.*, Vol. 25, (2001), pp. 425–432.
- [10] R. Kniep, H. Engelhardt and C. Hauf: “A First Approach to Borophosphate Structural Chemistry”, *Chem. Mater.*, Vol. 10, (1998), pp. 2930.
- [11] R. Kniep, G. Schäfer, H. Engelhardt and I. Boy: “K[ZnBP₂O₈] and A[ZnBP₂O₈] (A=NH₄⁺, Rb⁺, Cs⁺): Zincoborophosphates as a New Class of Compounds with Tetrahedral Framework Structures”, *Angew. Chem.* Vol. 38, (1999), pp. 3641–3644.
- [12] R.P. Bontchev, J. Do and A.J. Jacobson: “Templated Synthesis of Vanadium Borophosphate Cluster Anions”, *Angew. Chem.*, Vol. 38, (1999), pp. 1937–1940.
- [13] R.P. Bontchev, J. Do and A.J. Jacobson: “Synthesis and Characterization of the Layered Vanadium Borophosphate

- (Imidazolium)_{3,8}(H₃O)_{1,2}[(VO)₄(BO)₂(PO₄)₅]·0.3H₂O”, *Inorg. Chem.*, Vol. 39, (2000), pp. 3320–3324.
- [14] S.C. Sevov: “Synthesis and Structure of CoB₂P₃O₁₂(OH)·C₂H₁₀N₂: The First Metal Borophosphate with an Open Framework Structure”, *Angew. Chem.*, Vol. 35, (1996), pp. 2630–2632.
- [15] R. Kniep and G. Schäfer: “Isotype Borophosphate M^{II}(C₂H₁₀N₂)[B₂P₃O₁₂(OH)] (M^{II} = Mg, Mn, Fe, Ni, Cu, Zn): Verbindungen mit Tetraeder-Schichtverbänden”, *Z. Anorg. Allg. Chem.*, Vol. 626, (2000), pp. 141–147.
- [16] G.G. Schäfer, H. Borrmann and R. Kniep: “M^{II}(C₄H₁₂N₂)[B₂P₃O₁₂(OH)] (M^{II} = Co, Zn): Synthesis and Crystal Structure of Novel Open Framework Borophosphates”, *Z. Anorg. Allg. Chem.*, Vol. 627, (2001), pp. 61–67.
- [17] W.H. Flanke and T.E. Whyte: *Perspectives in Molecular Sieve Science*, American Chemical Society, Washington, D.C., 1998, pp. 15–32.
- [18] S. Rosemarie: *Handbook of Molecular Sieves*, Van Nostrand Reinhold, New York, 1992.
- [19] C.J. Warren, C.R. Haushalter, D.J. Rose and J. Zubietta: “Three-Dimensional Organic/Inorganic Composite Materials: Hydrothermal Synthesis and Structural Characterization of the Open-Framework Oxovanadium Borophosphate [H₃NCH₂CH₂NH₃]₂[(VO)₅(H₂O){O₃POB(O)₂OPO₃}]₂·1.5H₂O”, *Chem. Mater.*, Vol. 9, (1997), pp. 2694–2696.
- [20] R. Kniep, H.G. Will, I. Boy and C. Röhr: “6₁ Helices from Tetrahedral Ribbons 1∞ [BP₂O₈³⁻]: Isostructural Borophosphates M^IM^{II}(H₂O)₂[BP₂O₈] · H₂O (M^I = Na, K; M^{II} = Mg, Mn, Fe, Co, Ni, Zn) and Their Dehydration to Microporous Phases M^IM^{II}(H₂O)[BP₂O₈] (p 1013-1014)”, *Angew. Chem. Int. Ed. Engl.*, Vol. 36(9), (1997), pp. 1013–1014.
- [21] A. Yilmaz, X. Bu, M. Kızılyallı and G.D. Stucky: “Fe(H₂O)₂BP₂O₈·H₂O, a First Zeotype Ferriborophosphate with Chiral Tetrahedral Framework Topology”, *Chem. Mater.*, Vol. 12, (2000), pp. 3243–3245.
- [22] G. Schäfer, W. Carrillo-Cabrera, W. Schnelle, H. Borrmann and R. Kniep: “Synthesis and Crystal Structure of {(NH₄)_xCo_{((3-x)/2)}}(H₂O)₂[BP₂O₈] · (1 - x) H₂O (x ~ 0.5)”, *Z. Anorg. Allg. Chem.*, Vol. 628, (2002), pp. 289–294.
- [23] A. Baykal and M. Kızılyallı: “X-ray powder diffraction and IR study of NaMg(H₂O)₂[BP₂O₈]·H₂O and NH₄Mg(H₂O)₂[BP₂O₈]·H₂O”, *J. Mater. Sci.*, Vol. 35, (2000), pp. 4621–4626.
- [24] W.E. Klee and G. Engel: “IR. Spectra of the Phosphate Ions in Various Apatites”, *J. Inorg. Nucl. Chem.*, Vol. 32, (1970), pp. 1837–1843.
- [25] K. Nakamoto: *Infrared Spectra of Inorganic and Coordination Compounds*, Plenum Press, New York, 1971.
- [26] S.D. Ross: *Inorganic Infrared and Raman Spectra*, McGraw-Hill Press, London, 1972.
- [27] A. Baykal and M. Kızılyallı: “Synthesis and Characterisation of Anhydrous Magnesium Phosphate Mg₃(PO₄)₂”, *Turk. J. Chem.*, Vol. 21(4), (1997), pp. 394–400.

- [28] J.C. Vedrine and F. Delennay (Ed.): *Characterisation of Heterogeneous Catalysts*, Dekker, New York, 1994.
- [29] W.S. Kijlstra, E.K. Poels, A. Blik, B.M. Weckhuysen and R.A. Schoonheyd: “Characterization of Al₂O₃-Supported Manganese Oxides by Electron Spin Resonance and Diffuse Reflectance Spectroscopy”, *J. Phys. Chem. B*, Vol. 101, (1997), pp. 309–316.
- [30] Y. Köseoğlu, F. Yıldız, J.V. Yakhmi, J. Qin, X. Chen and B. Aktas: “EPR Studies on BEDT- TTF Intercalated MnPS₃ Molecular Magnet”, *J. Magn. Magn. Mater.*, Vol. 416-418, (2003), pp. 258–259.